

# Network distribution of mitochondria and lipid droplets in human muscle fibres

Christopher S. Shaw · David A. Jones ·  
Anton J. M. Wagenmakers

Accepted: 29 September 2007 / Published online: 16 October 2007  
© Springer-Verlag 2007

**Abstract** The objective of the present study was to develop a combination of fluorescent stains that would allow visualisation of the network of mitochondria and lipid droplets (intramyocellular lipids or IMCL) in human skeletal muscle fibres by means of conventional and confocal microscopy. Muscle biopsies were taken from the vastus lateralis of three lean, healthy and physically active male subjects. Frozen muscle sections were stained for mitochondria using antibodies against three mitochondrial proteins; porin, cytochrome *c* oxidase (COX) and NADH-ubiquinol oxidoreductase and neutral lipids were stained with oil red O. Anti-COX staining produced images with the strongest fluorescence signal and the highest resolution of the mitochondrial network and this stain was successfully combined with the antibody against type I fibre myosin. A highly organised matrix arrangement of mitochondria within the sarcomeres (in pairs at the I-band) was observed in the oxidative type I fibres. The density of mitochondria was the highest in the subsarcolemmal region. Anti-COX staining was combined with oil red O demonstrating that in type I fibres lipid droplets are mainly located in the space between the mitochondria.

**Keywords** Mitochondria · Intramyocellular lipids · Fluorescence · Confocal imaging · Skeletal muscle

## Introduction

Although the majority of lipid in the body is stored in adipose tissue a small amount is also stored within skeletal muscle fibres as lipid droplets. Biochemical extraction (Stellingwerf et al. 2007; Watt et al. 2002), tracer methodology (van Loon et al. 2001), immunohistochemistry (van Loon et al. 2003) and magnetic resonance spectroscopy (Schrauwen-Hinderling et al. 2003; de Bock et al. 2007) techniques have all demonstrated that these intramyocellular lipids (IMCL) are an important substrate that contributes significantly to total fat oxidation during exercise in physically active lean individuals (for review see van Loon 2004). However, obese insulin resistant individuals exhibit lower rates of fatty acid oxidation (Kim et al. 2000) and they appear unable to oxidise intramuscular lipid deposits during exercise (van Loon et al. 2005). It has been hypothesised that impairments in intramuscular lipid oxidation along with increased fatty acid availability in obese subjects will result in the accumulation of lipid metabolites [long-chain acylCoA (LCACoA), diacylglycerols (DAG) and ceramides] which have been implicated in the development of insulin resistance in muscle (Shulman 2000; Yu et al. 2002; Itani et al. 2001, 2002).

Koopman et al. (2001) developed a method to quantitatively analyse fibre type specific IMCL content in skeletal muscle using the lipid stain Oil Red O combined with immunofluorescence. Such a technique is required when measuring the use of IMCL during exercise as the reduction in IMCL is specific to type I fibres and may be missed using biochemical techniques which are unable to discriminate between fibre types and have a large coefficient of variation for total IMCL content in repeated biopsies (van Loon 2004; Watt et al. 2002).

C. S. Shaw · D. A. Jones · A. J. M. Wagenmakers (✉)  
Exercise Metabolism Research Group,  
School of Sport and Exercise Sciences,  
The University of Birmingham, Edgbaston,  
Birmingham B15 2TT, UK  
e-mail: A.Wagenmakers@bham.ac.uk

C. S. Shaw  
e-mail: css044@bham.ac.uk

Several studies utilising transmission electron microscopy (TEM) have demonstrated that the lipid droplets in muscle are preferentially located in the spaces immediately adjacent to the mitochondria, presumably so that they are readily oxidised during exercise (Hoppeler 1999; Tarnopolsky et al. 2006). Skeletal muscle mitochondria form a highly organised network (Kayar et al. 1988b) with the highest density being present in the subsarcolemmal (SS) regions especially adjacent to capillaries (Kayar et al. 1988a) and around nuclei (Kuznetsov et al. 2006; Tarnopolsky et al. 2006). According to ultra-high-resolution scanning electron microscopy images (Ogata and Yamasaki 1997) intermyofibrillar (IMF) mitochondria are arranged in a highly organised pattern with the mitochondria situated between myofibrils and organised in pairs on either side of the Z line at the level of the I band (Ogata and Yamasaki 1997). In confocal mitochondria specific fluorescent images of intact rat muscle fibres a characteristic ‘crystal-like matrix’ pattern was observed (Vendelin et al. 2005) with regular distances between mitochondria both in the longitudinal and perpendicular direction.

A decline in mitochondrial density/morphology and function occurs in many disease states (Ritov et al. 2005) and also with ageing and is believed to be a contributing factor to the accumulation of lipids and the development of insulin resistance (Petersen and Shulman 2006). Therefore a technique to directly analyse the spatial organisation of the network of mitochondria and lipid droplets from human muscle biopsies in terms of content, distribution and colocalisation with the main lipid metabolising enzymes could be an important step forward. Such a technique could also be used to investigate the response to exercise and intracellular signalling events activating these enzymes by means of phosphorylation (using phosphospecific antibodies) and translocation (e.g. Prats et al. 2006). Further development of these techniques is required to generate new knowledge about the molecular mechanisms leading to insulin resistance and disease and in determining the effectiveness of potential therapeutic interventions such as exercise, lifestyle changes and metabolic drugs.

The aim of the present study was, therefore, to develop an immunofluorescent method to visualise the mitochondrial network in human muscle fibres that could be combined with stains to identify muscle fibre type and IMCL content. We targeted three mitochondrial proteins, porin which is an abundant transmembrane protein that forms voltage-dependent anion channels (De Pinto et al. 1987) and two membrane-bound protein complexes involved in oxidative phosphorylation, NADH-ubiquinol oxidoreductase and cytochrome *c* oxidase (COX).

## Materials and methods

### Muscle samples

Skeletal muscle samples were obtained from the vastus lateralis of three healthy lean male volunteers using the Bergstrom percutaneous needle technique (Bergstrom 1975). Samples were blotted to remove excess blood and dissected free from visible collagen or fat. The muscle biopsies were embedded in Tissue-Tek OCT Compound (Sakura Finetek Europe, Zoeterwoude, The Netherlands) and immediately frozen in liquid nitrogen-cooled isopentane (Sigma-Aldrich, Dorset, UK). Serial 5 µm sections were cut at –30°C and collected onto room temperature, uncoated glass slides (VWR International Ltd, Leicestershire, UK) and left to air dry for a minimum of 1 h before treatment. Initially cross-sections were used to stain mitochondria with three different antibodies. Subsequently longitudinal sections were cut to visualise the arrangement of mitochondria and IMCL in relation to the sarcomere structure of the fibres.

### Immunofluorescence staining

All chemicals were obtained from Sigma-Aldrich unless otherwise stated. Phosphate buffered saline (PBS, 137 mM sodium chloride, 3 mM potassium chloride, 8 mM disodium hydrogen phosphate and 3 mM potassium dihydrogen phosphate, pH of 7.4.) was used for the dilution of antibodies, reagents and for use in the washing steps of the protocol.

Briefly sections were fixed in 3.7% formaldehyde for 1 h, followed by 3 × 30 s washes in deionised water. The slides were then permeabilised in 0.5% triton-X 100 for 5 min followed by three, 5 min washes in PBS. Muscle samples were then incubated in appropriate primary antibodies in PBS for 30 min, followed by three, 5 min washes in PBS. Labelling of fibre type was performed by incubating sections with mouse anti-myosin type I fibres (A4.840 DSHB, developed by Dr. Blau). Three antibodies against mitochondria were tested; mouse monoclonal anti-porin, mouse monoclonal anti-OxPhos Complex I (NADH-ubiquinol oxidoreductase), and mouse monoclonal anti-OxPhos Complex IV (cytochrome *c* oxidase; COX) (all from Invitrogen, Paisley, UK). The samples were further incubated in appropriately targeted secondary fluorescent conjugated antibodies for 30 min, followed by three, 5 min washes in PBS. The secondary antibodies used were goat anti-mouse IgM 350, IgG<sub>1</sub> 488, IgG<sub>2a</sub> 488 and IgG<sub>2b</sub> 488 (Invitrogen). When investigating fibre type specific mitochondrial content both antibodies used were generated in mouse. Although the secondary antibodies were isotype

specific to the primary antibody (IgM and IgG<sub>2a</sub> for anti-myosin and anti-COX respectively) we employed the approach used by Granneman et al. (2007) and incubated the sections with the appropriate primary and secondary antibodies in a sequential order. Therefore the sections were treated with the primary and secondary antibodies for myosin before the antibodies for mitochondria. The success of this approach is dependent on applying saturating concentrations of the first secondary antibody against the first primary antigen, in this case GAMIgM 488 against anti-myosin. A control step was performed to eliminate the chance of cross-reaction between the pair of antibodies where one of the primary antibodies was omitted. In all cases this resulted in the removal of the fluorescent signal. The lipid staining method used the neutral lipid dye Oil Red O in combination with immunofluorescence as developed by Koopman and colleagues (Koopman et al. 2001; van Loon et al. 2003). Sections were incubated in an oil red O solution for 30 min followed by three 30 s rinses in deionised water and a 10 min rinse with slow running tap water. A working solution of oil red O was made up of 500 mg oil red O in 100 ml of 60% triethylphosphate, 12 ml of which was diluted to a working solution with 8 ml deionised water, before being filtered twice to remove oil red O crystals. Coverslips were mounted in a glycerol and mowiol 4–88 solution in 0.2 M Tris-buffer (pH 8.5) with the addition of 0.1% 1,4-diazobicyclo-[2,2,2]-octane (DABCO) antifade medium.

#### Fluorescence microscopy

Initial images comparing the effectiveness of the three mitochondrial stains and the initial fibre type-specific mitochondrial network distribution were captured using a Nikon E600 microscope coupled to a SPOT RT KE colour three shot CCD camera (Diagnostic Instruments Inc., MI, USA). In order to visualise the Alexa fluor 350 and 488 fluorophores the DAPI UV (340–380 nm) and FITC (465–495) excitation filters were used respectively. Sections stained with oil red O were examined using a Texas red (540–580 nm) excitation filter. Digital images showing the detailed structure of the mitochondrial network and the position of lipid droplets in longitudinal sections of muscle fibres were acquired with an inverted confocal microscope (Leica DMIRE2, Leica Microsystems) with a 63× oil immersion objective. Alexa fluor 488 fluorophore was excited with a 488 nm line of the argon laser for excitation and 510–550 nm emission. Oil red O was excited with the 514 nm line of the Helium–Neon laser for excitation and greater than 520 nm emission. Images used to investigate colocalisation of mitochondria and oil red O were captured sequentially. Images were processed using Image-Pro Plus 5.1 software (Media Cybernetics, MD, USA) and intensity

thresholds were selected to represent minimum values for lipid droplets and mitochondria and used uniformly for all images.

Each longitudinal muscle fibre image was divided into 5 µm wide segments from the sarcolemma to the interior of the fibre, and the total area and the area occupied by lipid/mitochondria in the segment were measured. Mitochondrial and lipid content was expressed as the area fraction by dividing the stained area in the fibre segment by the total area of that segment.

In order to make conclusions on the relative position of mitochondria and lipid droplets on both sides of the myofibrillar sub-bands we have compared our confocal (immuno)fluorescence images with historic Transmission Electron Micrograph (TEM) images from the historic files of Dr. David Jones made at University College London (Fig. 6). These interpretations are made in the discussion section.

#### Statistical analyses

To compare total mitochondria and total IMCL content in type I and type II muscle fibres, a paired samples *t*-test was performed. Comparisons of mitochondria and lipid content in successive 5 µm bands from the sarcolemma was performed using a one-factor repeated measures analysis of variance (ANOVA). Tukey post hoc tests were performed in the case of a significant *F* ratio. Statistical significance was set at *P* < 0.05. All data are expressed as mean ± SD.

#### Results

Figure 1 shows representative images of cross-sections of human skeletal muscle viewed with a standard immunofluorescence microscope following incubation with mitochondrial antibodies using a protocol of formaldehyde fixation and permeabilisation with Triton X-100 used previously for oil red O staining of IMCL by Koopman et al. (2001). The antibody against COX successfully stained mitochondria (Fig. 1) with clear staining between the myofibrils (IMF) in the deeper layers of the muscle fibres. In addition, large areas of intense fluorescence signal can be seen in some of the fibres immediately below the sarcolemma probably reflecting accumulations of densely packed SS mitochondria. Anti-porin (Fig. 1) showed a similar intense signal in the SS region of some of the muscle fibres but had a weaker IMF stain especially in the deeper layers of the muscle fibres in comparison to the COX antibody. The antibody against complex I of the respiratory chain (NADH-ubiquinol oxidoreductase) showed very weak staining in both regions (not shown). All subsequent staining of mitochondria was performed using anti-COX.

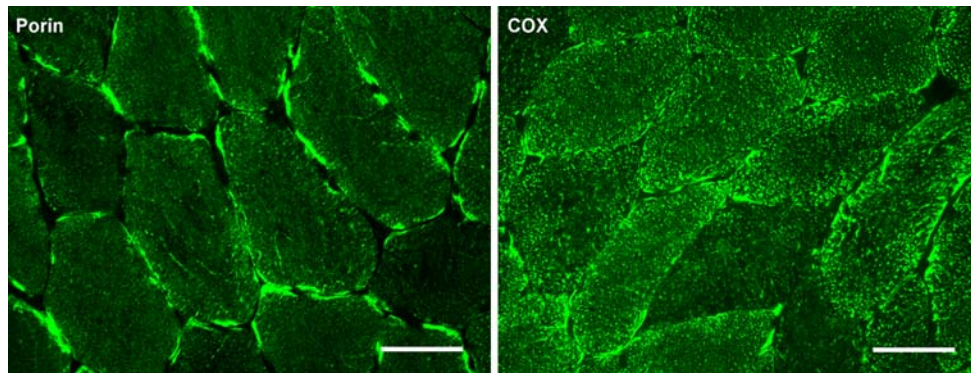


**Fig. 1** Conventional immunofluorescence microscopy to visualise mitochondria in human skeletal muscle using anti-porin (*left*) and anti-COX (*right*) (bars = 50  $\mu$ m). Note that both antibodies show an intense

signal in subsarcolemmal regions but anti-COX shows a stronger intracellular fluorescence signal in the deeper regions and better spatial resolution compared to anti-porin

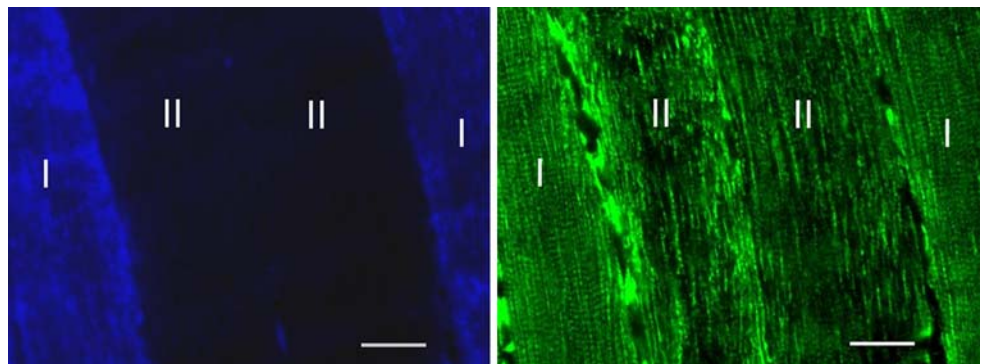
When the anti-COX mitochondrial stain was combined with anti-myosin type I and viewed with conventional fluorescence microscopy it became clear that the arrangement and density of the mitochondrial network differs between fibre types (Fig. 2).

When viewed with a confocal laser scanning microscope (CLSM), longitudinal muscle sections of the type I fibres showed a highly organised pattern, with mitochondria placed at regular intervals both perpendicularly and longitudinally to the fibre axis (Fig. 3). In the longitudinal direction the mitochondria appear to be arranged in a line which is divided by a series of black lines running at right angles to the axis of the fibre. Towards the edges of the fibre the mitochondria appear to fuse together to form a continuous line spanning several sarcomeres. Accumulations of densely packed mitochondria are seen in the type I fibre immediately below the sarcolemma (4). The type II fibres demonstrated a less structured pattern in comparison to type I fibres (Fig. 4) in that they were not in an ordered pattern perpendicular to the axis of the fibre. It is also notable that there are fewer pairs of mitochondria in the type II fibres and areas in which there were no or very few mitochondria. In both fibres, the density of IMF mitochondria was higher in regions close to the sarcolemma (Fig. 4).

Quantitative image analysis demonstrated that total mitochondrial content (expressed as area fraction stained) was greater in type I fibres compared to type II fibres ( $0.172 \pm 0.020$  vs.  $0.098 \pm 0.015$  respectively,  $P < 0.05$ ). When the mitochondrial content was quantified in successive 5  $\mu$ m bands from the sarcolemma towards the interior of the fibre, both type I and type II fibres showed the greatest mitochondrial content in the segment closest to the sarcolemma which gradually decreased towards the interior of the fibre ( $0.282 \pm 0.085$  vs.  $0.124 \pm 0.036$  and  $0.138 \pm 0.064$  vs.  $0.066 \pm 0.026$  for type I and type II fibres respectively,  $P < 0.05$ ). The difference between type I and II fibres was most notable in the immediate SS region (0–5  $\mu$ m).

Figure 3 shows IMCL visualised using CLSM on longitudinal muscle sections in the IMF (Fig. 3) and SS regions (Fig. 3) of type I fibres. Lipid droplets associated with IMF mitochondria were located in a similar way to the distribution of the mitochondria in that they are seen along the length of the muscle fibre although there are more gaps in the matrix distribution than seen with the mitochondria. Figure 3 demonstrates that IMCL are also associated with the accumulations of mitochondria in the SS region. Image analysis of the IMCL content and distribution demonstrated that type I fibres have the greater content (expressed as area fraction stained)

**Fig. 2** Double immunofluorescence staining to visualise fibres with slow myosin (type I), stained blue (*left*) and mitochondria, stained green (*right*) on longitudinal muscle sections (bars = 20  $\mu$ m). Note the more regular mitochondrial network, higher mitochondrial density and clear cross-striations in the type I fibres



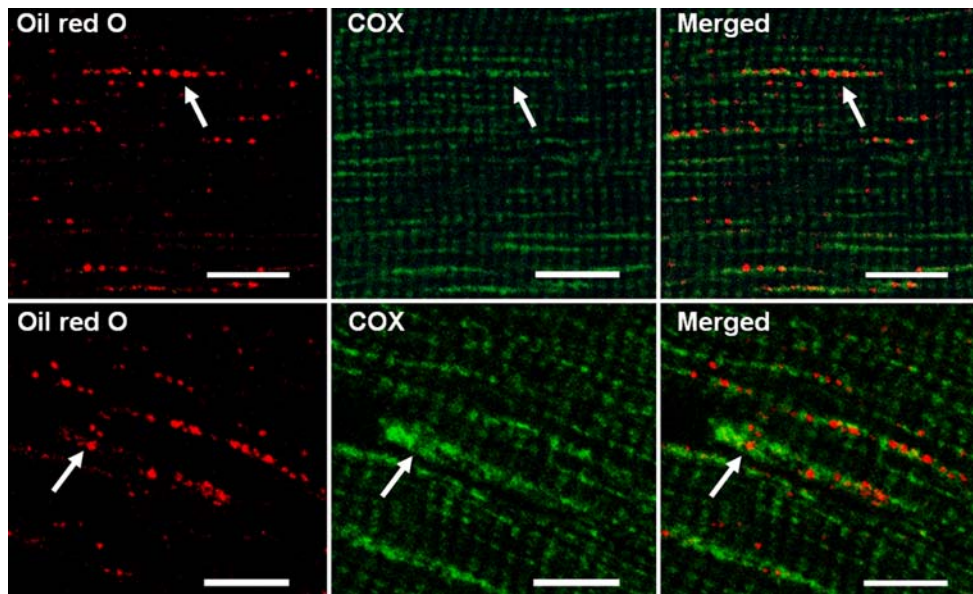


**Fig. 3** Confocal image of a longitudinal section of a type I muscle fibre stained for anti-COX and intramyocellular lipid droplets in the interior of the fibre (*upper panel*) and in areas around the sarcolemma (*lower panel*) (bars = 10  $\mu\text{m}$ ). Note that when images are merged the lipid droplets appear to be in the space between the intermyofibrillar mitochondria (*upper panel*, *arrow*). Comparison with TEM images

(Fig. 6) suggests that the mitochondria are oriented in pairs at the I-band. Only part of the spaces between neighbouring IMF mitochondria are filled with lipid droplets. Dense accumulations of mitochondria with a small number of lipid droplets are also visible in some areas immediately below the sarcolemma (*lower panel*, *arrow*)

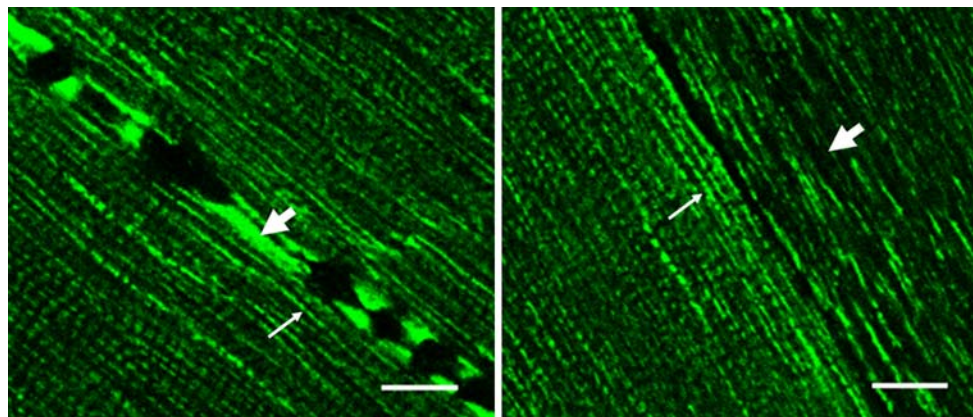


**Fig. 4** Confocal image of mitochondrial arrangement in two type I fibres (*left image*) and comparison of the mitochondrial arrangement in a type I fibre (on *left*) and type II fibre (on *right*) (*right image*) (bars = 10  $\mu\text{m}$ ). The distribution pattern of the intermyofibrillar mitochondria in the type I fibres (*left image*) is highly ordered. Areas with dense accumulations of mitochondria can be seen in the subsarcolem-

mal region of the fibres (*large arrow*, *left image*). Note the greater density and apparent interconnections of IMF mitochondria near the cell border (*small arrows*). Also note the irregular distribution of mitochondria and large areas without mitochondria in the fast fibres (*right image*, *large arrow*) and the lower mitochondrial density in comparison to the slow fibres especially in subsarcolemmal regions

of IMCL ( $0.029 \pm 0.010$  and  $0.014 \pm 0.006$  for type I and type II respectively,  $P < 0.05$ ). The IMCL content in the area immediately below the sarcolemma was higher ( $0.036 \pm 0.015$  for type I and  $0.021 \pm 0.009$  for type II fibres) in comparison to central region of the fibre ( $0.025 \pm 0.009$  for type I and  $0.010 \pm 0.006$  for type II fibres) (Fig. 5b). Combining the Oil Red O stain for lipids with anti-COX (Fig. 3) allows the position of individual lipid droplets to be observed in relation to the mitochondria. This demonstrates that the lipid droplets are mainly situated in the

space between mitochondria and in very close contact to them. Only a small fraction of the available lipid positions is occupied, implying that the network density of IMCL is lower than that of the mitochondria in trained muscles.

## Discussion

In this study we describe a method to identify fibre type specific differences in the network distribution of mitochon-

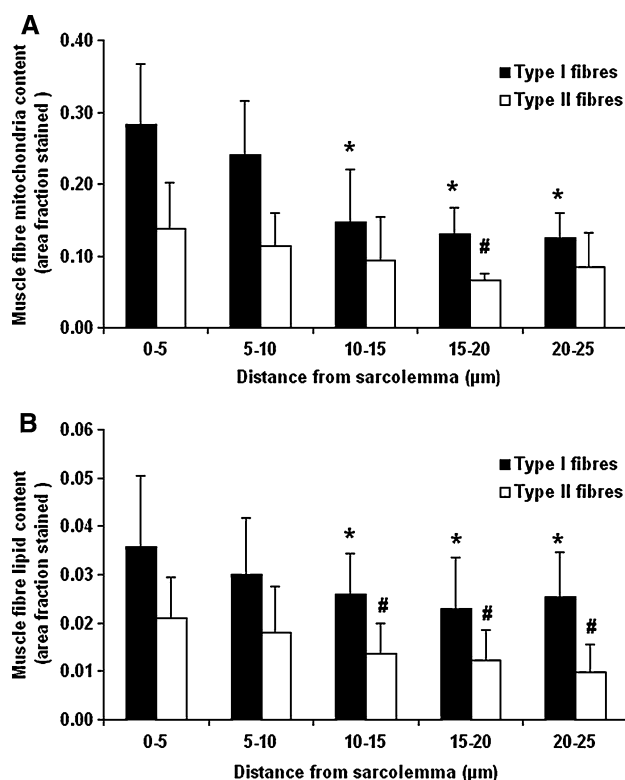


**Fig. 5** Type I and type II muscle fibre mitochondria (a) and intramyocellular lipid (b) content (expressed as area fraction stained) in successive 5 µm bands from the sarcolemma towards the interior of longitudinal muscle fibres. Data are mean ± SD. Twelve type I and type II muscle fibres were randomly selected from a longitudinal muscle preparation and analysed for the mitochondria and lipid content. \*Significantly different from subsarcolemmal region (0–5 µm) in type I fibres, #significantly different from subsarcolemmal region in type II fibres,  $P < 0.05$

dria and IMCL within human muscle fibres using traditional and confocal (immuno)fluorescence microscopy. The methodology combines the use of antibodies against complex IV of the respiratory chain (COX) with a previously established method to stain IMCL with oil red O. As far as we are aware this is the first time that the combined network of mitochondria and lipid droplets has been identified on longitudinal sections of frozen human muscle using this method. Previous attempts to visualise the mitochondrial network in rat muscle (Hashimoto et al. 2005) and in human muscle (He et al. 2004) with (immunofluorescence) microscopy were applied to muscle cross-sections which do not provide information on the longitudinal alignment of the mitochondria and IMCL.

The spatial distribution of mitochondria and IMCL within muscle fibres has previously been investigated in human and animal muscle fibres using TEM (Howald et al. 1985; Kayar et al. 1988a, b; Tarnopolsky et al. 2006). TEM also visualises myofibrils and, therefore, is complimentary to the current method to determine the position of mito-

chondria and IMCL along the sub-bands of the myofibrils. However, TEM visualises only a small section within a muscle fibre and, therefore, is unlikely to represent the mean network distribution in type I and type II fibres in a given muscle of a given individual. The immunofluorescence method described here covers many fibres in one preparation, and, therefore gives a better representation of the entire muscle. This is particularly important when comparing differences between subject groups (e.g. trained vs. sedentary) and for the interpretation of the physiological consequences of such differences. Quantitation of the fractional mitochondrial content using this fluorescent confocal technique produces distribution patterns throughout the fibre (Fig. 5) similar to those previously observed with EM (Howald et al. 1985; Kayar et al. 1988a). However the fractional content that we report is about two-fold higher than classical stereological estimates of volume fraction with EM (Kayar et al. 1988a; Tarnopolsky et al. 2006; Vock et al. 1996). The most likely causes of this are overprojection of light to areas adjacent to the mitochondrial border and because of section thickness. This implies that the method for the time being is only semiquantitative for estimates of volume fraction and this may explain the difference with values obtained with the ‘gold standard’ EM method.

The images obtained with anti-COX on longitudinal sections (Fig. 2), especially those with confocal microscopy (Figs. 3, 4) show an ordered structure of the mitochondria particularly in type I fibres. The mitochondria are arranged along the longitudinal axis of the fibre and with a clear cross-striation pattern. When comparing these images with conventional EM pictures (Fig. 6) the mitochondria seem to occupy the spaces between myofibrils primarily in the I band region often with pairs of mitochondria on either side of the Z line. The dark spaces in the line of mitochondria (as in Figs. 3, 4) seem to correspond to the A band. In some instances, and especially towards the edge of the fibres, the lines of mitochondria coalesce and clearly extend beyond the I band to include the A band as well. Our interpretation of the images is consistent with previous work on intact rat muscle fibres using confocal fluorescence microscopy (Kuznetsov et al. 2006; Vendelin et al. 2005) and also with ultra-high-resolution scanning electron microscope images of individual fixed human muscle fibres (Ogata and Yamasaki 1997). This distribution of the IMF mitochondria has been suggested to facilitate ATP-diffusion, keeping to a minimum the distance between mitochondria, the adjacent sarcomere, T-tubules and enzymes involved in the process of substrate utilisation and muscle contraction (Kuznetsov et al. 2006; Vendelin et al. 2005).

Densely packed accumulations of mitochondria were also seen in the SS regions (Fig. 4). In agreement with EM work of Howald et al. (1985) in humans these accumula-

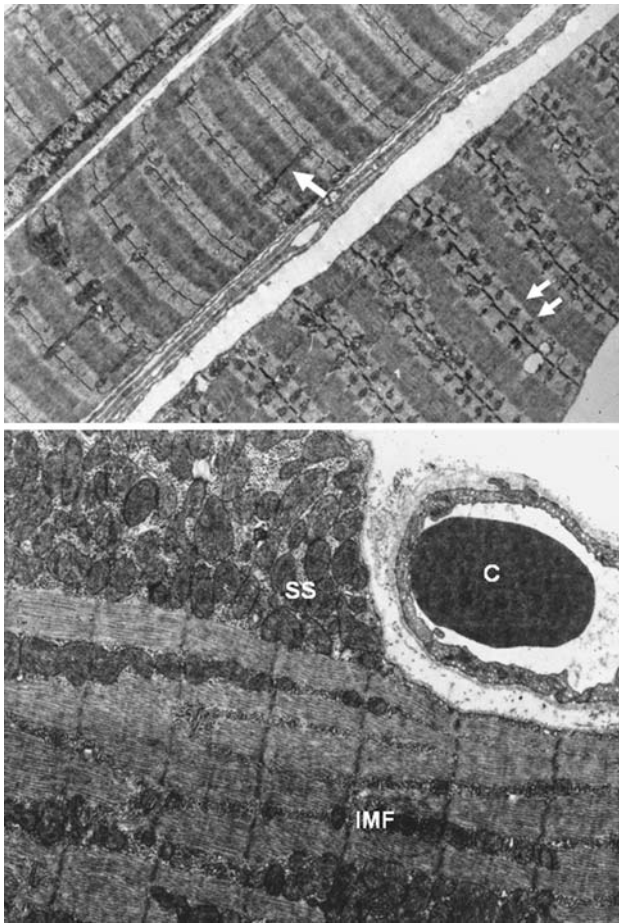


**Fig. 6** Transmission electron micrographs showing mitochondria in longitudinal muscle fibres. Both images are from a historic file of David A Jones and made at University College London. Two fibres from mouse extensor digitorum longus muscle (*upper image*) showing pairs of mitochondria at the I band level between the myofibrils. The fibre on the right is probably a slow twitch fibre (based on the thickness of the Z lines) and shows a high density of mitochondria in a regular pairwise arrangement (*double arrow*). Fast twitch fibre on the left shows a lower density of mitochondria, with mitochondria only occasionally being seen on both sides of the Z line. Also note interconnected mitochondria that extend over the A band (*arrow*). Human vastus lateralis muscle (*lower image*) showing densely packed areas of subsarcolemmal mitochondria (*SS*) adjacent to a capillary (*C*) and also the inter-connected lines of intermyofibrillar mitochondria between myofibrils near the cell border (*IMF*)

tions were more common in type I fibres. Previous EM work in various species also suggested that these accumulations of mitochondria are frequently seen in areas adjacent to capillaries (Fig. 6) and in perinuclear regions (Kayar et al. 1988a; Kuznetsov et al. 2006; Tarnopolsky et al. 2006).

The mitochondrial stain on longitudinal sections also combined successfully with the IMCL stain using oil red O fluorescence (Fig. 3). The combined images show that the lipid droplets are in close proximity to the IMF mitochondria. This is consistent with TEM observations of Hoppeler

(1999), Tarnopolsky et al. (2006) and Vock et al. (1996). The lipid droplets according to the TEM images occupy the gaps between adjacent mitochondria in the A band region on both sides of the sarcomere. There is evidence that the close proximity of lipid droplets and mitochondria may have a functional relationship in that it allows the lipids to be hydrolysed and oxidised efficiently during exercise (Hoppeler 1999; Tarnopolsky et al. 2006). van Loon et al. (2003) have suggested that only the IMCL in type I fibres (all close to the mitochondria as shown in Fig. 3) are oxidised during exercise in trained subjects. Stellingwerf et al. (2007) observed greater depletion during exercise of the IMCL in the region under the sarcolemma than those in the centre of the fibre. Tarnopolsky et al. (2006) using EM demonstrated that the number of lipid droplets in direct contact with the mitochondria can be increased through regular exercise.

The present study is the first to show that IMCL and mitochondria have a similar pattern of distribution in human muscle with the highest density in SS regions and a progressive decline in deeper regions (Fig. 5a, b). The same IMCL distribution has been observed before in trained human muscle by Stellingwerf et al. (2007) but without measurement of the mitochondrial density. A higher density of mitochondria within sarcolemmal regions with a progressive decline towards the central regions was previously observed with EM in horse (Kayar et al. 1988a) and with fluorescence in rat fibres (Kuznetsov et al. 2006).

A different arrangement of the distribution network of mitochondria and IMCL in obese and patient populations compared to the lean active subjects in this study could play an important role in the development of insulin resistance and type II diabetes. A lower content of total mitochondria (Holloway et al. 2007), a very low content of IMF mitochondria in the SS region (Ritov et al. 2005) and a lipid distribution shift with a higher lipid content in the centre of the muscle fibres (Malenfant et al. 2001) have all been observed in the muscle of obese subjects and could lead to a physical separation of mitochondria and IMCL and contribute to the accumulation of fatty acid metabolites. The combined staining technique on longitudinal muscle fibres developed in this study can be ideally used to investigate whether the physical separation of mitochondria and lipid droplets is larger in the distribution network observed in the muscle of obese and patient populations.

In conclusion, we have successfully developed a new staining method suited to investigate the spatial 'crystal-like matrix' distribution of mitochondria and IMCL in type I and type II human muscle fibres using confocal immunofluorescence microscopy. The new method provides information on the network distribution of mitochondria and IMCL that are compatible with and extend what has been learned previously from EM images in several species. The

new method is more flexible and less time consuming and allows more fibres to be examined in a single biopsy sample than EM. This should facilitate future studies investigating the important link between lipid metabolism, exercise training and insulin resistance in obesity and the metabolic syndrome.

**Acknowledgments** The antibody against myosin (human slow fibres, A4.840) used in the study was developed by Dr. Blau and was obtained from the Developmental Studies Hybridoma Bank developed under the auspices of the NICHD and maintained by The University of Iowa, Department of Biological Sciences, Iowa City, IA 52242.

## References

- Bergstrom J (1975) Percutaneous needle biopsy of skeletal muscle in physiological and clinical research. *Scand J Clin Lab Invest* 35:609–616
- De Bock K, Dresselaers T, Kiens B, Richter EA, van Hecke P, Hespel P (2007) Evaluation of intramyocellular lipid breakdown during exercise by biochemical assay, NMR spectroscopy, and oil-red-oil staining. *Am J Physiol Endocrinol Metab* doi:10.1152/ajpendo.00112.2007
- De Pinto V, Ludwig O, Krause J, Benz R, Palmeri F (1987) Porin pores of mitochondrial outer membranes from high and low eukaryotic cells: biochemical and biophysical characterization. *Biochim Biophys Acta* 894:109–119
- Granneman JG, Moore HPH, Granneman RL, Greenberg AS, Obin MS, Zhu Z (2007) Analysis of lipolytic protein trafficking and interactions in adipocytes. *J Biol Chem* 282:5726–5735
- Hashimoto T, Masuda S, Taguchi S, Brooks GA (2005) Immunohistochemical analysis of MCT1, MCT2, and MCT 4 expression in rat plantaris muscle. *J Physiol* 567:121–129
- He J, Goodpaster BH, Kelley DE (2004) Effects of weight loss and physical activity on muscle lipid content and droplet size. *Obese Res* 12:761–769
- Hoppeler H (1999) Skeletal muscle substrate metabolism. *Int J Obes Relat Metab Disord* 23:S7–S10
- Holloway GP, Thrush AB, Heigenhauser GJF, Tandon NN, Dyck DJ, Bonen A, Spriet LL (2007) Skeletal muscle mitochondrial FAT/CD36 content and palmitate oxidation are not decreased in obese women. *Am J Physiol Endocrinol Metab* 292:E1782–E1789
- Howald H, Hoppeler H, Claassen H, Mathieu O, Straub R (1985) Influences of endurance training on the ultrastructural composition of the different muscle fiber types in humans. *Pflugers Arch* 403:369–376
- Itani SI, Pories WJ, MacDonald KG, Dohm GL (2001) Increased protein kinase C theta in skeletal muscle of diabetic patients. *Metabolism* 50:553–557
- Itani SI, Ruderman NB, Schneider F, Boden G (2002) Lipid-induced insulin resistance in human muscle is associated with changes in diacylglycerol, protein kinase C, and I $\kappa$ B- $\alpha$ . *Diabetes* 51:2005–2011
- Kayar SR, Hoppeler H, Essen-Gustavsson B, Schwerzmann K (1988a) The similarity of mitochondrial distribution in equine skeletal muscles of differing oxidative capacity. *J Exp Biol* 137:253–263
- Kayar SR, Hoppeler H, Mermod L, Weibel ER (1988b) Mitochondrial size and shape in equine skeletal muscle: a three-dimensional reconstruction study. *Anat Rec* 222:333–339
- Kim JY, Hickner RC, Cortright RL, Dohm GL, Houmard JA (2000) Lipid oxidation is reduced in obese human skeletal muscle. *Am J Physiol Endocrinol Metab* 279:E1039–E1044
- Koopman R, Schaart G, Hesselink MKC (2001) Optimisation of oil red O staining permits combination with immunofluorescence and automated quantification of lipids. *Histochem Cell Biol* 116:63–68
- Kuznetsov AV, Troppmair J, Sucher R, Hermann M, Saks V, Margreiter R (2006) Mitochondrial subpopulations and heterogeneity revealed by confocal imaging: possible physiological role? *Biochimica Biophys Acta* 1757:686–691
- Malenfant P, Joannisse DR, Theriault R, Goodpaster BH, Kelley DE, Simoneau JA (2001) Fat content in individual muscle fibers of lean and obese subjects. *Int J Obes Relat Metab Disord* 25:1316–1321
- Ogata T, Yamasaki Y (1997) Ultra-high-resolution scanning electron microscopy of mitochondria and sarcoplasmic reticulum arrangement in human red, white and intermediate muscle fibres. *Anatomical Rec* 248:214–223
- Petersen KF, Shulman GI (2006) Etiology of insulin resistance. *Am J Med* 119:10S–16S
- Prats C, Donsmark M, Qvortrup K, Londres C, Sztalryd C, Holm C, Galbo H, Ploug T (2006) Decrease in intramuscular lipid droplets and translocation of HSL in response to muscle contraction and epinephrine. *J Lipid Res* 47:2392–2399
- Ritov VB, Menshikova EV, He J, Ferrell RE, Goodpaster BH, Kelley DE (2005) Deficiency of subsarcolemmal mitochondria in obesity and type 2 diabetes. *Diabetes* 54:8–14
- Schrauwen-Hinderling VB, van Loon LJC, Koopman R, Nicolay K, Saris WHM, Kooi ME (2003) Intramyocellular lipid content is increased after exercise in nonexercising human skeletal muscle. *J Appl Physiol* 95:2328–2332
- Shulman GI (2000) Cellular mechanisms of insulin resistance. *J Clin Invest* 106:171–176
- Stellingwerf T, Boon H, Jonkers RAM, Senden JM, Spriet LL, Koopman R, van Loon LJC (2007) Significant intramyocellular lipid use during prolonged cycling in endurance trained males as assessed by three different methodologies. *Am J Physiol Endocrinol Metab* 292:E1715–E1723
- Tarnopolsky MA, Rennie CD, Robertshaw HA, Fedak-Tarnopolsky SN, Brose AN, Devries MC, Hamadeh MJ (2006) The influence of endurance exercise training and sex on intramyocellular lipid and mitochondrial ultrastructure. *Am J Physiol Regul Integr Comp Physiol* 292:R1271–R1278
- van Loon LJC (2004) Use of intramuscular triacylglycerol as a substrate source during exercise in humans. *J Appl Physiol* 97:1170–1187
- van Loon LJC, Greenhaff PL, Constantin-Teodosiu D, Saris WHM, Wagenmakers AJM (2001) The effects of increasing exercise intensity on muscle fuel utilisation in humans. *J Physiol* 536:295–304
- van Loon LJC, Koopman R, Stegen JHCH, Wagenmakers AJM, Keizer HA, Saris WHM (2003) Intramyocellular lipids form an important substrate source during moderate intensity exercise in endurance-trained males in a fasted state. *J Physiol* 553:611–625
- van Loon LJC, Manders RJF, Koopman R, Kaastra B, Stegen JHCH, Gijzen AP, Saris WHM, Keizer HA (2005) Inhibition of adipose tissue lipolysis increases intramuscular lipid use in type 2 diabetic patients. *Diabetologia* 48:2097–2107
- Vendelin M, Beraud N, Guerrero K, Andrienko T, Kuznetsov AV, Olivares J, Kay L, Saks VA (2005) Mitochondrial regular arrangement in muscle cells: a “crystal-like” pattern. *Am J Physiol Cell Physiol* 288:C757–C767
- Vock R, Hoppeler H, Claassen H, Wu DXY, Billeter R, Weber J, Taylor CR, Weibel ER (1996) Design of the oxygen substrate pathways. VI. Structural basis of intracellular substrate supply to mitochondria in muscle cells. *J Exp Biol* 199:1689–1697
- Watt MJ, Heigenhauser GJF, Spriet LL (2002) Intramuscular triacylglycerol utilization in human skeletal muscle during exercise: is there a controversy? *J Appl Physiol* 93:1185–1195
- Yu C, Chen Y, Cline GW, Zhang D, Zong H et al (2002) Mechanism by which fatty acids inhibit insulin activation of insulin receptor substrate-1 (IRS-1)-associated phosphatidylinositol 3-kinase activity in muscle. *J Biol Chem* 277:50230–50236